

Effect of compounding and plastic processing methods on the development of bioplastics based on acetylated starch reinforced with sugarcane bagasse cellulose fibers

Perla Rosa Fitch-Vargas^a, Irma Leticia Camacho-Hernández^b,
Francisco Javier Rodríguez-González^c, Fernando Martínez-Bustos^d, Abraham Calderón-Castro^b,
José de Jesús Zazueta-Morales^b, Ernesto Aguilar-Palazuelos^{b,*}

^a Facultad de Ciencias del Mar, Universidad Autónoma de Sinaloa, Paseo Claussen S/N, Col. Los Pinos, 82000 Mazatlán, Sinaloa, Mexico

^b Posgrado en Ciencia y Tecnología de Alimentos, Facultad de Ciencias Químico-Biológicas, Universidad Autónoma de Sinaloa, Cd. Universitaria, Av. de las Américas y Josefa Ortiz S/N, 80010 Culiacán, Sinaloa, Mexico

^c Centro de Investigación en Química Aplicada, Blvd. Enrique Reyna 140, 25100 Saltillo, Coahuila, Mexico

^d Centro de Investigación y de Estudios Avanzados, Libramiento Norponiente, Fracc. Real de Juriquilla, 76230 Querétaro, Mexico

ARTICLE INFO

Keywords:

Bioplastics
Acetylated starch
Cellulose fibers
Compounding
Plastics processing

ABSTRACT

Fiber-reinforced starch-based bioplastics provide an excellent alternative to synthetic materials for packaging. Hence, it is important to develop materials based on starch and natural fibers on an industrial scale. The effect of compounding thermoplastic acetylated corn starch (TPAS)/sugarcane bagasse cellulose fibers (SF) biocomposites using both single and twin-screw extruders (SSE and TSE) and the effect of plastic processing methods such as compression molding, injection molding, and flat film extrusion on physical properties of starch-based bioplastics were studied. Bioplastics were characterized using AFM, XRD, SEM, rheometry, tensile tests, water-solubility, contact angle, and weight loss during soil burial. Compounding the TPAS/SF biocomposites by TSE resulted in a significant decrease in the fiber length and a more homogeneous distribution of SF in the TPAS matrix than SSE. The biocomposite processing by injection reduced the fiber's length even more and improved the SF distribution and mechanical properties. The biomaterials' solubility ranged from 24.9% to 28.2%, which is lower than native starch-based biocomposites. Therefore, it was possible to develop TPAS/SF bioplastics on an industrial scale to be an alternative to conventional plastics.

1. Introduction

Due to the environmental pollution caused by petroleum-based plastics and fossil resource dependency, there is interest in developing biodegradable materials. Starch is considered one of the most promising biopolymers for producing sustainable materials owing to its biodegradability, low cost, abundance, and renewability (Amin et al., 2019). The processing and applications of native starch are limited since it is

not a natural thermoplastic, which generates a melting point higher than the degradation temperature. In the presence of a plasticizer (glycerol, sorbitol, among others) and specific processing conditions, the starch granules are fragmented, swelled, and melted, resulting in a material with thermoplastic properties (thermoplastic starch, TPS) (Alves-Da Silva et al., 2020; Rico et al., 2016). TPS has significant disadvantages, such as high water sensibility, high viscosity, and low mechanical properties. These drawbacks could be improved by blending TPS with

Abbreviations: TPAS, thermoplastic acetylated corn starch; SF, sugarcane bagasse cellulose fibers; AFM, atomic force microscopy; ANOVA, analysis of variance; Com, compression molding; CA, contact angle; FF, flat film extrusion; FTIR, fourier-transform infrared spectroscopy analysis; Inj, injection molding; RC, relative crystallinity; RH, relative humidity; SSE, single-screw extruder; SEM, scanning electron microscopy; TPS, thermoplastic starch; TSE, twin-screw extruder; WL, weight loss; WS, water solubility; XRD, x-ray diffraction.

* Correspondence to: Posgrado en Ciencia y Tecnología de Alimentos, Facultad de Ciencias Químico-Biológicas, Universidad Autónoma de Sinaloa, Cd. Universitaria, Av. de las Américas y Josefa Ortiz S/N, 80010 Culiacán, Sin., Mexico.

E-mail addresses: perlafitch@uas.edu.mx (P.R. Fitch-Vargas), camacho@uas.edu.mx (I.L. Camacho-Hernández), francisco.rodriguez@ciqa.edu.mx (F.J. Rodríguez-González), fmartinez@cinvestav.mx (F. Martínez-Bustos), abcalcas@uas.edu.mx (A. Calderón-Castro), zazuetaj@uas.edu.mx (J.J. Zazueta-Morales), eaguilar@uas.edu.mx (E. Aguilar-Palazuelos).

<https://doi.org/10.1016/j.indcrop.2022.116084>

Received 3 August 2022; Received in revised form 19 October 2022; Accepted 1 December 2022

Available online 6 December 2022

0926-6690/© 2022 Elsevier B.V. All rights reserved.

other natural polymers, reinforcing it with natural fibers, and modifying starch (Amin et al., 2019; Chaves da Silva et al., 2018; Huang et al., 2020). Acetylation is a chemical modification in which hydrophobic acetyl groups substitute a part of starch's hydroxyl groups. Acetylated starch presents lower water affinity, decreased gelatinization temperature, better thermoplasticity than native starch, and diminished retrogradation tendency (Colussi et al., 2017).

Sugarcane bagasse is an abundant agro-industrial residue of the sugar industry. Every year, approximately 57 million Tons of sugarcane are produced in Mexico, from which about 15 million tons are bagasse. The use of this biomass for the development of bioplastics has attracted significant attention due to its availability and renewable and ecological characteristics (Maldonado-García et al., 2018; Mandal and Chakraborty, 2011). Some researchers have reported that adding natural fibers, such as sugarcane fiber, to starch-based bioplastics enhances their mechanical and thermal properties and reduces the water affinity (Fitch-Vargas et al., 2019; Mohan et al., 2018). Nonetheless, despite the structural similarity between starch and cellulose, fiber surface modification is usually necessary; the most employed chemical methods are bleaching, alkali, and acetylation (Wang et al., 2014). The fiber surface treatments modify the fiber wettability and can remove non-cellulosic components and increase the fraction of cellulose exposed and reaction sites, improving the mechanical interlocking between TPS-fibers (Cao et al., 2006; Guimarães-de Farias et al., 2017; Li et al., 2007).

On the other hand, one of the main problems of producing starch-based bioplastics is their limited production on an industrial scale. Most studies on the development of starch-based bioplastics employ the casting method (CM) as a processing technique. CM is a lab-scale process that is difficult to scale up since it requires evaporation of a high water amount, and extended drying times are needed scale (Castillo et al., 2019; González-Seligra et al., 2017; Kim et al., 2014). Furthermore, thermal starch processing is complex due to its multiphase transitions, e. g., water diffusion, expansion of granules, gelatinization, melting, decomposition, and crystallization in a limited temperature range (González-Seligra et al., 2017). Therefore, it is essential to develop TPS-based materials using conventional technologies for plastics processing, such as extrusion, injection molding, compression molding, and flat film, among others, to understand better the starch behavior and its processing challenges at an industrial. Before obtaining bioplastics, a compounding stage is required to obtain homogeneous biocomposites (Fowler et al., 2006). Compounding can be performed by extrusion. This technology involves mechanical and thermal energy and has many advantages, such as excellent mixing, low infrastructure cost, and operational flexibility (Rico et al., 2016). Moreover, based on the number of screws, extruders can be classified as single-screw or twin-screw extruders (SSE and TSE, respectively). Depending on the compounding system, SSE or TSE, and processing conditions, the fiber-reinforced starch-based bioplastics' structural properties and possible applications could be influenced (Altskär et al., 2008; Castillo et al., 2019; Ochoa-Yepes et al., 2019). Thus, it is important to study the compounding stage to obtain bioplastics with good mechanical, physical, and microstructural properties.

In the last years, several authors have developed biomaterials by employing conventional technologies for plastics processing, obtaining promising results (Alves-Da Silva et al., 2020; Castillo et al., 2019; Zanela et al., 2018). Lenz et al. (2018) evaluated the effect of up to 10 reprocessing cycles in fiber-reinforced corn starch-based biocomposites. Ochoa-Yepes et al. (2019) studied the influence of extrusion/thermo-compression and lentil protein content on starch films. While Chaves da Silva et al. (2018) produced starch-recycled gelatine films employing flat extrusion. Nonetheless, there are no reports about the study of compounding stage and plastic technologies in developing bioplastics based on acetylated starch reinforced with sugarcane bagasse cellulose fibers. Hence, it was hypothesized that it is possible to obtain fiber-reinforced starch-based bioplastics on an industrial scale. Likewise, TSE's compounding will probably generate a

more intense mixing and better dispersion, improving the biomaterials' mechanical properties.

In previous research, biocomposites based on acetylated corn starch (TPAS), sugarcane bagasse cellulose fibers (SF), and glycerol were obtained (Fitch-Vargas et al., 2019). It was found that the chemical modification of both starch and sugarcane bagasse helped obtain biocomposites with enhanced functional properties and water resistance. By the above, this work aims to obtain bioplastics from a blend of TPAS, SF, and glycerol and evaluate the effect of compounding and plastic processing methods (injection molding, compression molding, and flat film extrusion) on their physical properties.

2. Materials and methods

2.1. Materials

Acetylated corn starch (E14320, Ingredion, USA) with humidity of $8.2 \pm 0.4\%$, and $\text{pH} = 5.3 \pm 0.1$, was supplied by Paxell S.A. de CV (Querétaro, Mexico). The methodology proposed by Jeon et al. (1999) was used to evaluate the degree of substitution (DS) of acetylated corn starch (TPAS), obtaining a value of $0.08 \pm 0.02\%$. Glycerol was obtained from JT Baker® (PA, USA).

Sugarcane bagasse (lignin= $12.1 \pm 0.6\%$, hemicellulose= $14.6 \pm 0.6\%$, cellulose= $48.0 \pm 0.3\%$) was donated by the Sugarmill El Dorado S.A. de C.V. (Culiacán, Sinaloa, México). The sugarcane bagasse was chemically treated by alkalization, bleaching, and acetylation to remove the non-cellulosic components, following the methodology proposed by Fitch-Vargas et al. (2019). The sugarcane bagasse cellulose fibers (SF) (lignin= $0.8 \pm 0.1\%$, hemicellulose= 2.5% , cellulose= $84.1 \pm 0.1\%$) were stored at $25 \pm 2^\circ\text{C}$ before being employed as reinforcement for the TPAS.

2.2. Methods

2.2.1. Compounding

In a reported work from this group, a biocomposite with good functional properties was obtained by the plasticization of TPAS (64%) with 24% glycerol and reinforcement with 12% SF (Fitch-Vargas et al., 2019). In order to evaluate the effect of the melt mixing environment on the processability and performance of the TPAS/SF bioplastics, two compounding systems were compared. On the one hand, the blend was processed by a single screw extruder (Davis-Standard, Pawcatuck, CT, USA) having a mixing head. A temperature profile of $65\text{--}80\text{--}85^\circ\text{C}$ and a screw speed of 50 rpm were used. Materials were cut and dried at 50°C for 24 h in a convection oven (**single-screw extruded biocomposites, SSE**). On the other hand, the blend was processed in a twin-screw extruder (Werner & Pfleiderer ZSK30, Ramsey, NJ, USA), having an $L/D = 29$. A temperature profile of $80\text{--}85\text{--}85\text{--}85\text{--}85^\circ\text{C}$ was used. Feed and screw rates were kept constant at 14 g/min and 50 rpm, respectively. The final product was pelletized and dried for 24 h at 50°C (**twin-screw extruded biocomposites, TSE**). The biocomposites extruded in both compounding systems were maintained at a relative humidity (RH) of 53% before being used.

2.2.2. Starch-based bioplastics

2.2.2.1. Injection molding. Injection-molded samples for tensile tests (ASTM D638) of the TPAS/SF biocomposites were prepared using a Fu Chun Shin Injector (HT150, Tainan City, Taiwan). A temperature profile of $115\text{--}130\text{--}140\text{--}140^\circ\text{C}$ and a screw speed of 38 rpm was employed. Specimens of TPAS/SF biocomposites showed a thickness of 3.2 ± 0.1 mm.

2.2.2.2. Compression molding. 40 g of the TPAS/SF biocomposites were placed into $150 \times 150 \times 3$ mm molding plates and compression-molded

using two pneumatic presses (PHI 023OH-X4A, CA, USA), the first for heating at 125 °C and the second for cooling at 25 °C. A pressure of 15 tons was applied for 6 min throughout the melting, followed immediately by the cooling press with a pressure of 15 tons. Sheets of TPAS/SF biocomposites showed a thickness of 1.5 ± 0.1 mm.

2.2.2.3. Flat extrusion. Flat films of the TPAS/SF biocomposites were obtained using a single-screw extruder (Killion Model KTS-100, NJ, USA) having an $L/D = 24$ and a compression ratio of 3:1 and equipped with a mixing head and a 30×0.5 mm flat die. The biocomposites were extruded at 50 rpm using a temperature profile of 100–120–130–140–140 °C. Flat films were cooled and stretched using a chill roll having a final thickness of 0.5 ± 0.1 mm.

The injected, compressed, and flat film biocomposites (Fig. SD-1) were conditioned at 25 °C and 53% RH for 48 h until their characterization.

2.2.3. Characterization

2.2.3.1. Atomic force microscopy (AFM). Atomic force micrographs were obtained at contact mode using a Bruker Innova microscope (Bruker Corp., MA, USA). A scanning speed of 0.5 Hz per line of 128 pixels and samples of 5×5 μm were used. The surface roughness parameters R_a (Roughness average), R_q (Root mean square roughness), Kurtosis, and Skewness were calculated from AFM images. Each biomaterial was analyzed in triplicate.

2.2.3.2. X-ray diffraction (XRD). Sheets of TPAS/SF bioplastics and ground raw material (TPAS and SF) were packed into a glass container with a depth of 0.5 mm and placed on an X-ray diffractometer (Rigaku Model Last D/Max-2100, Rigaku Denki Co. Ltd., Japan). Diffractograms were obtained by using a sweep angle of Bragg of 5–60 ° over a scale of 2 θ with intervals of 0.02, operating at 30 kV and 16 mA, with a wavelength $\lambda = 1.5406$ Å and CuK α radiation. The relative crystallinity (RC) was calculated according to Herman's method (Wang et al., 2017).

2.2.3.3. Fourier-transform infrared spectroscopy analysis (FTIR). FTIR analysis was performed to detect functional groups in the raw material and bonding interactions in bioplastics. Spectra were obtained using an FTIR spectrometer (Nicolet™ iS™ 50, Thermo Fisher Scientific Co., Waltham, MA, USA.). The samples' FTIR spectra were recorded in 4000–400 cm^{-1} at a scan rate of 32 and spectral resolution of 4 cm^{-1} . FTIR spectrum was employed in transmittance.

2.2.3.4. Scanning electron microscopy (SEM). The morphology observations of longitudinal and cross-section of TPAS/SF biocomposites were performed using a scanning electron microscope (Philips®, Model XL30 ESEM, Eindhoven, Holland) with a secondary electron detector and 15 kV of acceleration. Samples were fractured in liquid nitrogen and spread with gold for observation. Microphotographs were obtained by ESEM XL-30 software. The raw material and bioplastics fiber lengths were measured from the micrographs dimensions (at 100 and 250X), and an average of 20 replicates was reported (Fig. SD2-SD4).

2.2.3.5. Oscillatory rheometry. Complex viscosity (η^*), storage modulus (E'), and loss modulus (E'') of TPAS/SF biocomposites compounded by SSE and TSE were determined following the methodology of Rodriguez-Gonzalez et al. (2004). A modular and compact oscillation rheometer (MOD PHYSICA MCR 301, Anton Paar, Graz, Austria) coupled to a heating chamber and 25 mm plate-plate geometry was employed. Measurements were performed at 140 and 150 °C and a frequency range of 0.5–50 Hz with an amplitude of 0.1% by duplicate.

2.2.3.6. Mechanical properties. Tensile tests were evaluated using an MTS Criterion® texturometer (Model 43, Eden Prairie, MN, USA)

according to ASTM D-882 and ASTM D638 standard methods for flat films and injection samples, and compression-molded samples, respectively. Eight replicates were made per treatment.

2.2.3.7. Water solubility (WS). The WS of TPAS/SF bioplastics indicates their integrity in an aqueous medium. WS was determined according to Ochoa-Yepes et al. (2019). Samples of 2 cm diameter were dried at 100 °C for 24 h to record the initial dry weight. Dried were immersed in water for 24 h at 25 °C and dried at 100 °C for 24 h to obtain the final dry weight. Four measurements per type of bioplastic were done.

2.2.3.8. Contact angle. A goniometer (Model NRL CA 100–00, Ramé-Hart Instrument Co., NJ, USA) was employed to measure the water contact angle and the hydrophobicity of the surface of the TPAS/SF bioplastics (Li et al., 2018). The sample was fixed on a stainless steel sheet using double-sided tape. A drop of distilled water (10 μL) was placed on the surface of the samples using a Hamilton micro-syringe (Model 80000, NV, U.S.A), and immediately the images were captured. This procedure was repeated four times per treatment.

2.2.3.9. Weight loss (WL). The soil burial method was performed to calculate the WL of bioplastics as an indirect measure of biodegradability. The methodology is an adaptation of the proposed by Kaith et al. (2010) and Ibrahim et al. (2018). Samples of 15×15 mm were buried at a depth of 10 cm in a mixture of 50% soil and 50% worm humus. Materials were kept at 25 ± 2 °C and with an RH of $75 \pm 5\%$. Three samples per treatment were washed with distilled water and dried at 60 °C for 24 h every week. The WL was determined for five weeks.

2.2.4. Statistical analysis

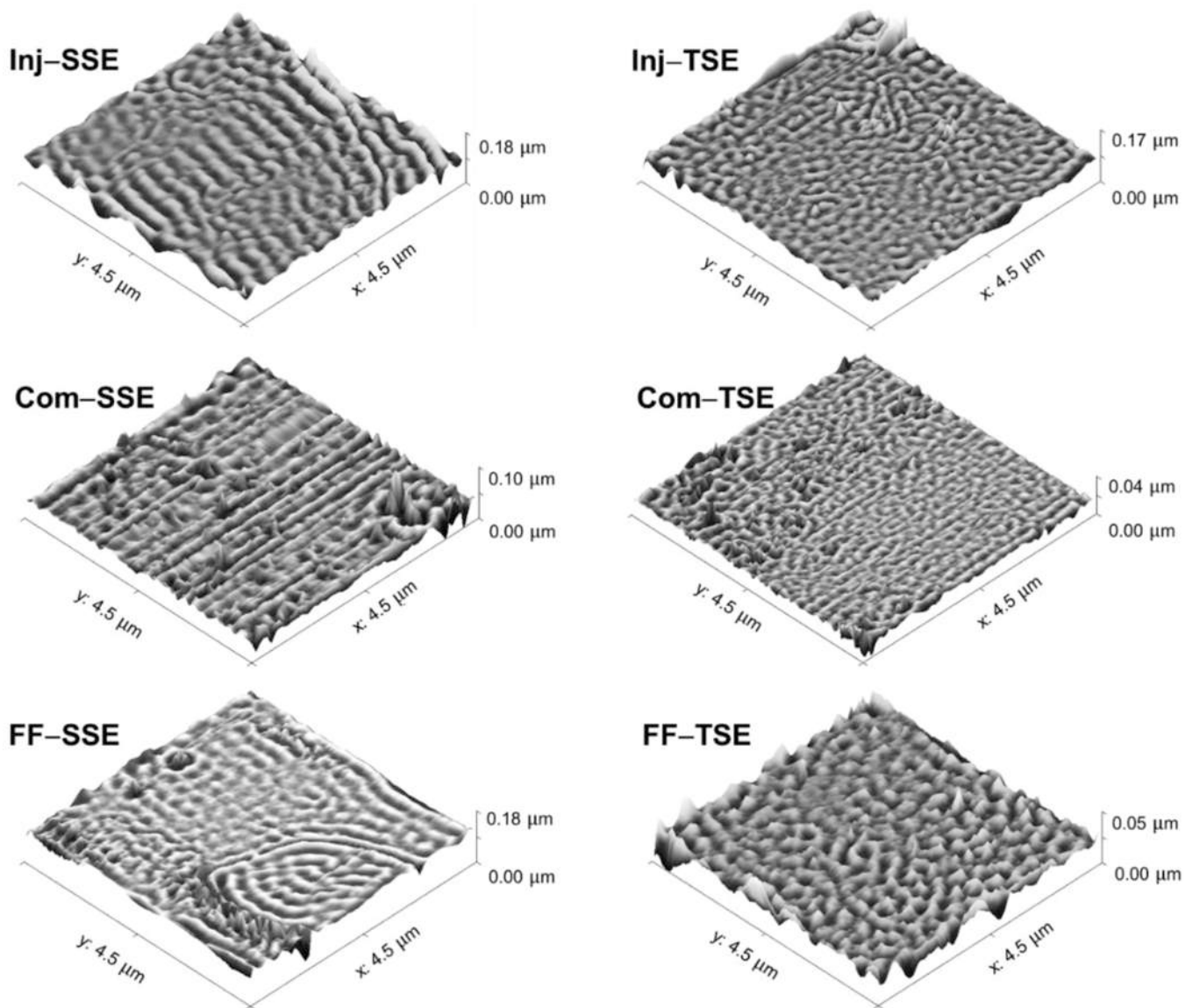
For data analysis, a completely randomized factorial design was performed. Factor A was the compounding process; meanwhile, Factor B was the plastic processing method. The levels of Factor A were single-screw extrusion (SSE) and twin-screw extrusion (TSE), whereas Factor B levels were injection molding (Inj), compression molding (Com), and extrusion of flat films (FF). There were six treatments, Inj–SSE, Inj–TSE, Com–SSE, Com–TSE, FF–SSE, and FF–TSE. Data statistical analysis was performed through analysis of variance (ANOVA) with Statgraphics plus 6.0 (Manugistics, Rockville, MD, USA). Means were compared using the Tukey test with a 95% confidence level.

3. Results and discussion

3.1. AFM

As observed by AFM, the surface roughness could indirectly be used to measure fiber dispersion in the starch matrix and to estimate interaction forces. Fig. 1 displays the AFM images and roughness parameters of TPAS/SF bioplastics compounded by SSE and TSE and processed by Inj, Com, and FF. It is observed that TSE compounding presented a more uniform three-dimensional surface with a lower number of agglomerations compared to SSE due to a suitable fibers dispersion and hydrogen bonding forming between TPS and fibers. It has been reported that during the compounding stage, an adequate fiber dispersion promotes good interfacial adhesion, avoids voids, and ensures a complete immersion in the polymeric matrix, where TSE provides a more intensive mixing and mechanical damage than SSE (Lenz et al., 2018; Pickering et al., 2016). In addition, R_q was lower for the materials compounded by TSE. Li et al. (2020) reported that a decreased R_q indicates better dispersion of the bioplastics' components.

Albrektsson and Wennerberg (2004) defined classification for the surface roughness of materials based on the values of R_a : 0–0.4 μm , 0.4–1.0 μm , 1.0–2.0 μm and > 2.0 μm for smooth, moderately rough, rough and highly rough, respectively. According to this scale, materials processed by Inj have a moderately rough surface. The roughness could



Treatment	Ra (nm)	Rq (nm)	Kurtosis	Skewness
Inj-SSE	523.4 ± 38.9	616.8 ± 43.9	-0.510 ± 0.1	-0.159 ± 0.1
Inj-TSE	446.4 ± 238.7	530.8 ± 302.9	-0.935 ± 0.2	-0.163 ± 0.1
Com-SSE	329.6 ± 99.5	480.5 ± 119.1	-1.112 ± 0.1	-0.136 ± 0.2
Com-TSE	96.2 ± 33.8	118.9 ± 43.4	-0.243 ± 0.5	0.091 ± 0.5
Pp-SSE	411.6 ± 132.7	507.7 ± 146.1	-0.3159 ± 0.7	-0.306 ± 0.01
Pp-TSE	343.4 ± 112.6	421.2 ± 133.5	-0.426 ± 0.1	-0.251 ± 0.3

Fig. 1. Atomic force micrographs and roughness parameters of Inj-SSE, Inj-TSE, Com-SSE, Com-TSE, FF-SSE, and FF-TSE. SSE=Single screw extruder, TSE=Twin screw extruder, Inj=Injection molding, Com=Compression molding, FF=Flat film extrusion, Ra=Roughness average, Rq=Root mean square roughness.

depend on the processing conditions, such as the shear rate (Mohan et al., 2018). Com and FF are low-shear rate processes, and the samples showed smooth surfaces. Conversely, Inj is a high-shear rate process, and the high viscosity of the TPAS/SF biocomposites could produce a less smooth surface.

Skewness is a measure of the symmetry deviation of the surface. Negative skewness is related to deep valleys, while positive values show surfaces containing mainly asperities or peaks (Taaca and Vasquez Jr, 2017). The negative skewness values of the biomaterials suggest the

presence of holes in the surface. On the other hand, the kurtosis values measure the uniformity of surface variations. All treatments recorded negative values of kurtosis. According to Bajpai et al. (2018), kurtosis values less than three indicate a homogeneous distribution and relatively flat surfaces. Hence, bioplastics with homogeneous fibers dispersion were obtained despite the complexity of the starch processing due to multiphase transitions during thermal processing, where TSE showed the best performance (González-Seligra et al., 2017).

3.2. XRD

During the starch processing, its semi-crystalline structure is wholly or partially destroyed. After thermomechanical processing, two types of crystallinity can be detected: a) residual crystallinity (A, B, or C crystallinity produced by incomplete melting of starch) and b) processing-induced crystallinity, V_A (not hydrated), V_H (hydrated), and E_H . These changes are detected by XRD (Van Soest et al., 1996).

XRD patterns of TPAS, SF, and TPAS/SF bioplastics processed by Inj, Com, and FF are shown in Fig. 2. TPAS presented a diffractogram with four prominent peaks at values 2θ of 13.2° , 15.2° , 17.9° , and 23.1° , and relative crystallinity (RC) of 24.1%. SF showed three principal peaks at 15.8° , 22.4° , and 34.6° , with an RC of 70.5%. The materials showed a large amorphous halo and two diffraction peaks at 19.8° and 22.5° (2θ) (Wang et al., 2017). The V_H -type structure can be detected at 19.8° (2θ) and has been reported to occur during TPS processing due to the formation of complexes between amylose and glycerol (Van Soest et al., 1996). On the other hand, the peaks at around 22.4° (2θ) could be associated with crystalline planes (0 0 2) and (1 0 1) of the structure of cellulose-I (Motaung and Anandjiwala, 2015). Also, it has been reported that peaks at 22.5° could represent a type A pattern indicating that some native starch granules were not wholly gelatinized (Raquez et al., 2008).

The RC of all the TPAS/SF biomaterials ranged between 14.4% and

16.2%. These values could be related to the inherent crystallinity of cellulose and TPS and the possible formation of V_H -type structures during processing (Van Soest et al., 1996). In addition, due to the processing effect, the RC of biomaterials was significantly lower than the obtained for the unprocessed raw material. Depending on the processing conditions and residence time, there are changes in starch and fiber, like a decrease in fibers length, significant fragmentation of starch granules, and modification of their crystalline spectrums (Castillo et al., 2019; Van Soest et al., 1996; Wang et al., 2017). Nonetheless, no defined trend was detected on how specifically the compounding stage and plastic processing technologies affected the RC.

3.3. FTIR analysis

Fig. 3 shows the FTIR spectra of TPAS, SF, and TPAS/SF bioplastics. All samples recorded bands at $3281\text{--}3332\text{ cm}^{-1}$ (O–H group) and $2893\text{--}2929\text{ cm}^{-1}$ (C–H stretching vibration). The peak at 1645 cm^{-1} was associated with absorbed water (H_2O). The bands at 1150 and 1017 cm^{-1} correspond to C–O bond stretching. While the peaks at 859 , 759 , and 572 cm^{-1} could be due to the stretching vibration of the anhydroglucose ring (Guimarães-de Farias et al., 2017; Jumaidin et al., 2017; Ochoa-Yepes et al., 2019). Native starch and TPAS spectra are shown in Fig. SD-5. According to Olagunju et al. (2020), there is

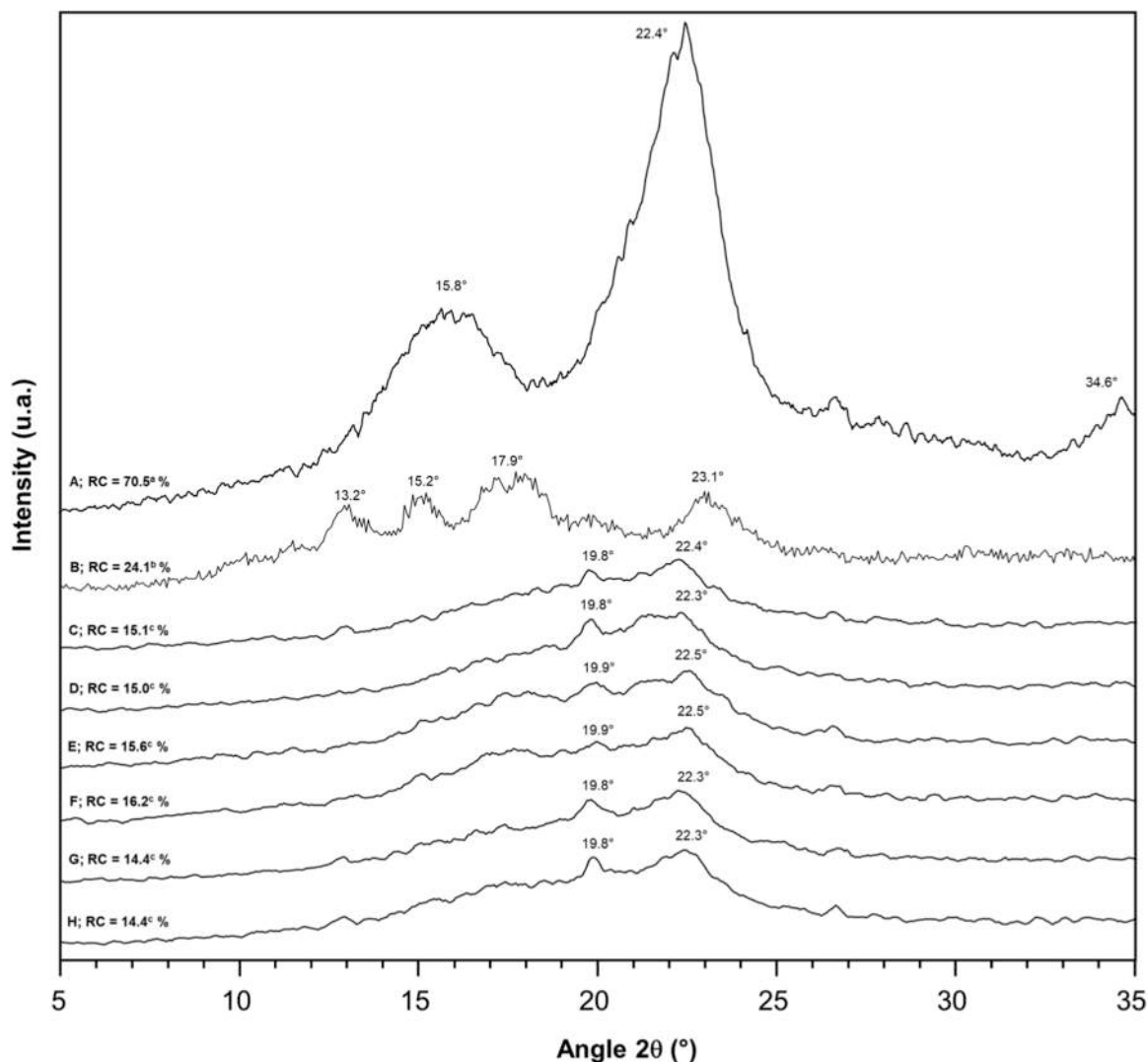


Fig. 2. XRD patterns and relative crystallinity (RC) for (A) SF, (B) TPAS, (C) Inj-SSE, (D) Inj-TSE, (E) Com-SSE, (F) Com-TSE, (G) FF-SSE and (H) FF-TSE. Different lowercase letters (a, b, c) show statistical differences ($P \leq 0.05$) among raw material and biomaterials according to the Tukey test.

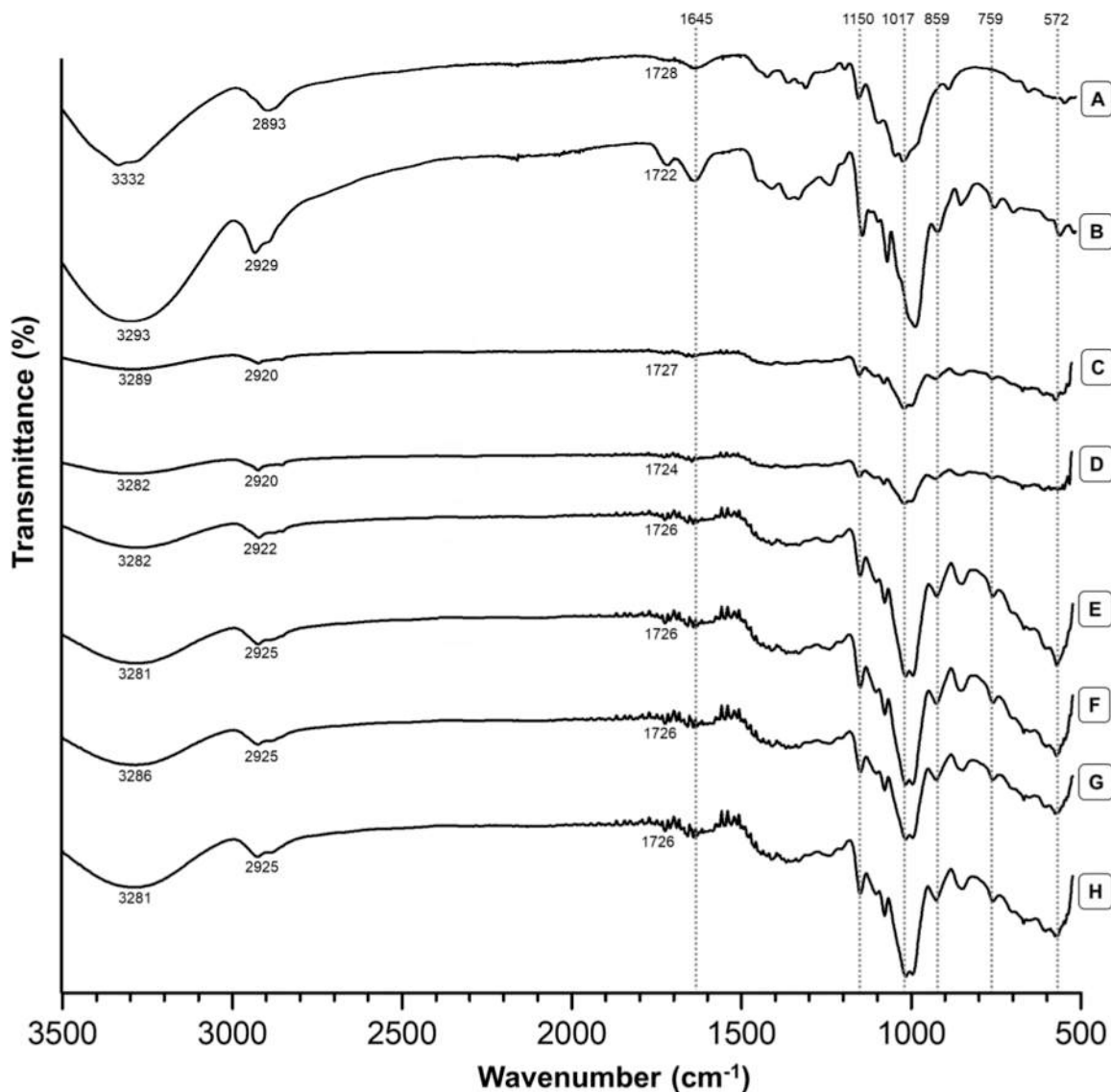


Fig. 3. FTIR spectra of (A) SF, (B) TPAS, (C) Inj-SSE, (D) Inj-TSE, (E) Com-SSE, (F) Com-TSE, (G) FF-SSE and (H) FF-TSE.

evidence of acetylation in the fingerprint region of $1800\text{--}800\text{ cm}^{-1}$. TPAS presented peaks not appreciated in native starch at 1722 cm^{-1} (C=O stretch) and 1245 cm^{-1} (C-C stretch). In addition, Fig. SD-6 shows that in the spectrum of unmodified sugarcane bagasse, peaks at 1604 , 1513 , and 1238 cm^{-1} (related to the hemicellulose and lignin) are not present in SF. It is known that fiber surface chemical treatments can remove compounds such as hemicellulose, lignin, waxes, and pectins. While the bands at 1159 , 1054 , 1030 , and 896 cm^{-1} , associated with the cellulose vibrations, showed an intensity increase in SF, suggesting that the chemical modification removed non-cellulosic compounds and increased the cellulose content (Cao et al., 2006; Guimarães-de Farias et al., 2017).

According to Jumaidin et al. (2017), the interactions among the biocomposites' components could be determined by identifying the bands' shift in the FTIR spectrum. The bands at $\approx 3281\text{--}3289\text{ cm}^{-1}$ (O-H group) of bioplastics shifted to a lower wavenumber compared to TPAS and SF (3293 y 3332 cm^{-1} , respectively), which could corroborate the hydrogen bonding interactions. Moreover, González-Seligra et al. (2016) propose that to compare the O-H groups available in samples, the intensity of the peaks at 3300 cm^{-1} (I_{3330}) and 1149 cm^{-1} (I_{1149}) could be associated. These peaks are related to C-O, and C-O-H stretching vibrations. The Inj specimens' intensity ratio (I_{3330}/I_{1149}) was

lower than Com and FF samples, indicating fewer available O-H groups. Hence, as an effect of the type of processing, it would be assumed that greater hydrogen bonding interactions are occurring in the injected molded materials.

3.4. SEM

Fig. 4A shows the sugarcane bagasse with fibers of $499.5 \pm 121.5\text{ }\mu\text{m}$ in length and arranged in stiff bundles due to the strong bonding of components such as cellulose, hemicellulose, lignin, and waxes. For its part, SF presented fibers of $251.3 \pm 65.5\text{ }\mu\text{m}$, a smaller diameter bundle and smoother surface (Fig. 4B); this may be a product of defibrillation and hemicellulose and lignin removal during the surface modification (Guimarães-de Farias et al., 2017).

The effect of compounding and processing equipment on the length of SF can be observed by comparing the SEM longitudinal-section micrographs of TPAS/SF biocomposites shown in Fig. 4C-F. The bioplastics processed by Com presented fibers of 241.3 ± 97.5 and $147.5 \pm 53.9\text{ }\mu\text{m}$ for Com-SSE and Com-TSE, respectively (Fig. 4E and F), while Inj-SSE and Inj-TSE presented fibers of 181.25 ± 50.3 and $70 \pm 19.4\text{ }\mu\text{m}$, respectively (Fig. 4C and D). It is quite evident that compounding in TSE produced a larger reduction in fiber length than that

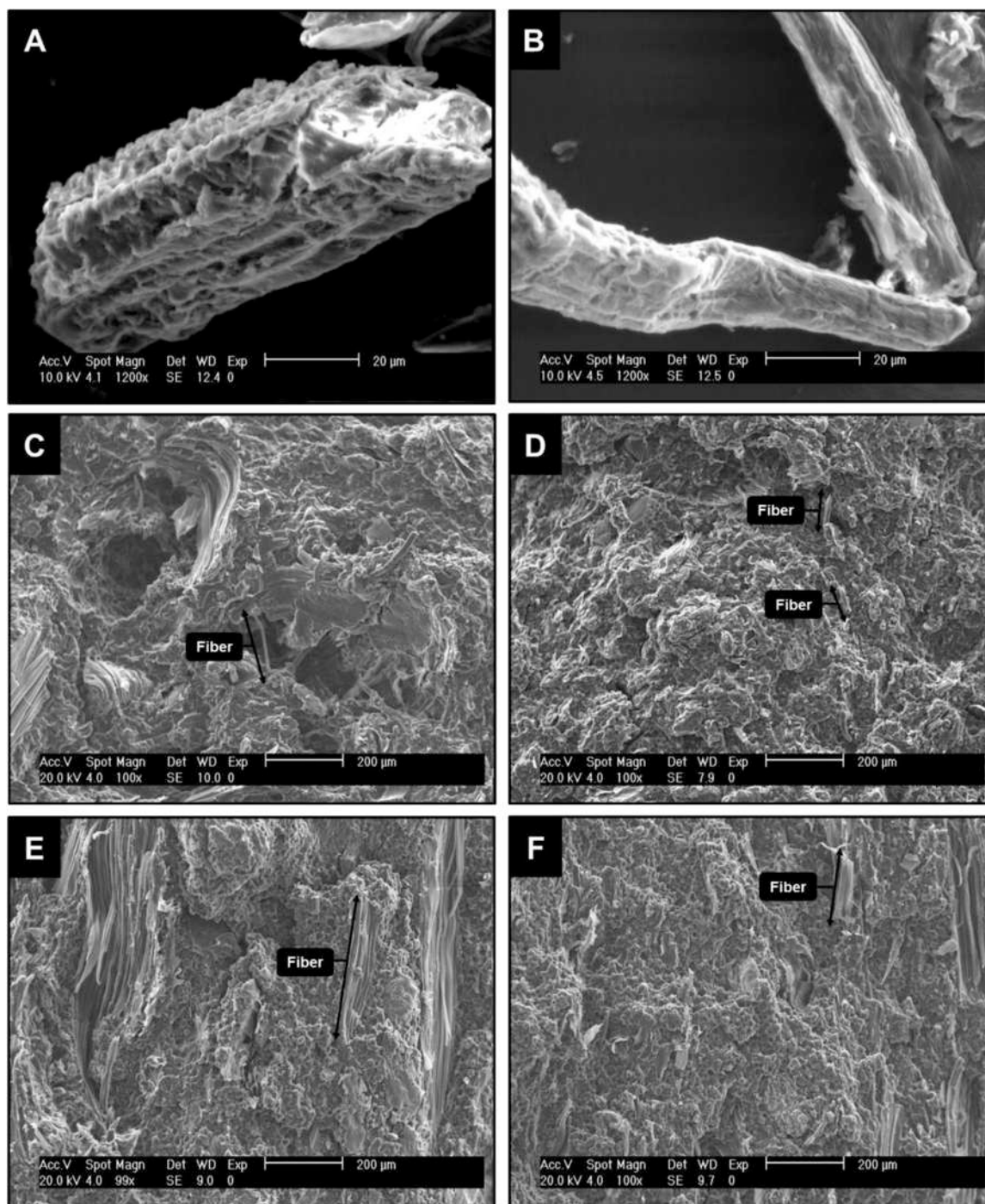


Fig. 4. SEM micrographs of (A) sugarcane bagasse and (B) SF at 1200x, (C) Inj-SSE, (D) Inj-TSE, (E) Com-SSE, and (F) Com-TSE at 100x.

observed after compounding in SSE. It has been widely reported that TSE provides more mechanical damage than SSE, promoting better dispersion (Lenz et al., 2018; Pickering et al., 2016). Moreover, the injection molding employs high temperatures and shear stress which decreased more the fiber length than processing by Com, where just heat is applied (Basiak et al., 2018; Li et al., 2018). Some authors report that wear improves the dispersion and orientation of fibers, thus providing better mechanical properties of the material (Gurunathan et al., 2015).

Fiber distribution in the biocomposites compounded by SSE (Fig. 4C and E) showed poor homogeneity, zones rich in TPAS, and poor in SF. In contrast, the biomaterials compounded by TSE presented a more homogeneous distribution of the SF in the TPAS matrix, which was

furtherly improved by the processing by Inj. From the above, it could be concluded that compounding by SSE and processing by Com resulted in less damage to SF but a poor distribution of fiber in the TPAS matrix. While compounding the TPAS/SF biocomposites by TSE and processing by Inj resulted in a good distribution of shorter fibers in the TPAS matrix.

Fig. 5 depicts 1000X micrographs of TPAS/SF biocomposites that shows a matrix of TPAS and smaller dispersed particles of SF than those observed in Fig. 4. The segments of the fibers exposed in the fractured samples showed a rough surface having a width larger than 20 μm, a thickness around four μm, and an exposed length up to 60 μm (Fig. 5C). The rough surface of SF was almost fully de-bonded from the TPAS matrix, but some small regions seemed to be bonded to the TPAS matrix

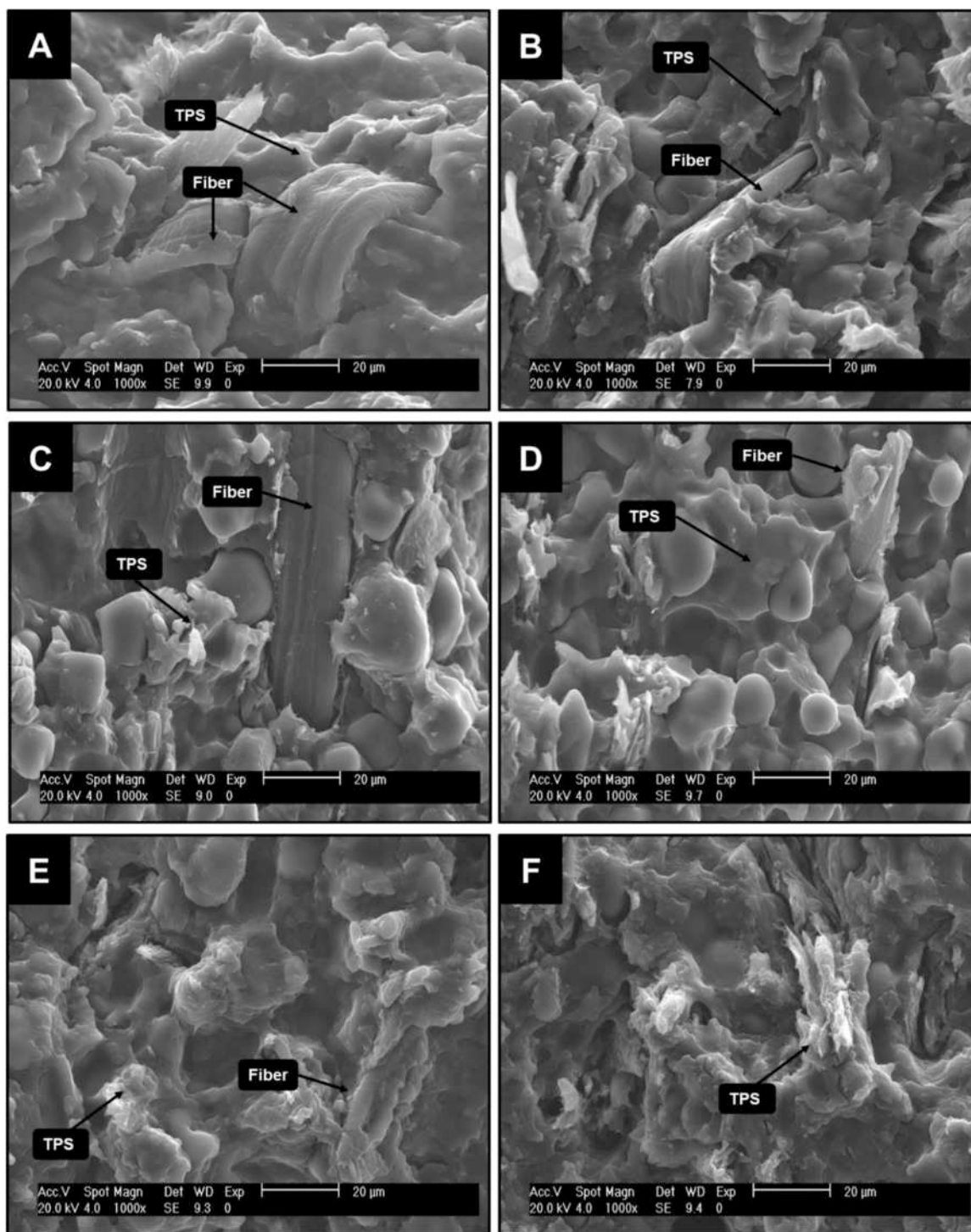


Fig. 5. SEM transversal-section micrographs of (A) Inj-SSE, (B) Inj-TSE, (C) Com-SSE, (D) Com-TSE, (E) FF-SSE and (F) FF-TSE (magnification at 1000X).

(Fig. 5B and C). Those small bonded regions were not large enough to allow the breakup of SF fibers at the level of the fracture surface. Bonded regions could be produced by the interactions between the acetylated segments of starch with the cellulose segments in the SF (Guimarães-de Farias et al., 2017).

3.5. Oscillatory rheometry

Fig. 6 shows the storage modulus (G'), loss modulus (G''), and complex viscosity (η^*) as a function of angular frequency (ω) of the biocomposites compounded in SSE and TSE and evaluated at 140 and

150 °C. All biocomposites showed a solid-like behavior evidenced by the almost frequency-independent values of G' and G'' and the fact that G' had higher values than G'' in the whole interval of frequencies (Rodríguez-Gonzalez et al., 2004). G' and G'' seemed to depend on temperature, i.e., the higher the testing temperature, the lower the values of G' and G'' . Moreover, biocomposites compounded in TSE showed higher values of G' and G'' at 140 °C than those compounded in SSE. It could be related to a better distribution of the fibers into the TPAS matrix, plasticization level, or starch degradation.

On the other hand, the η^* of the biocomposites also showed a pseudoplastic behavior. As expected, it was observed that as the

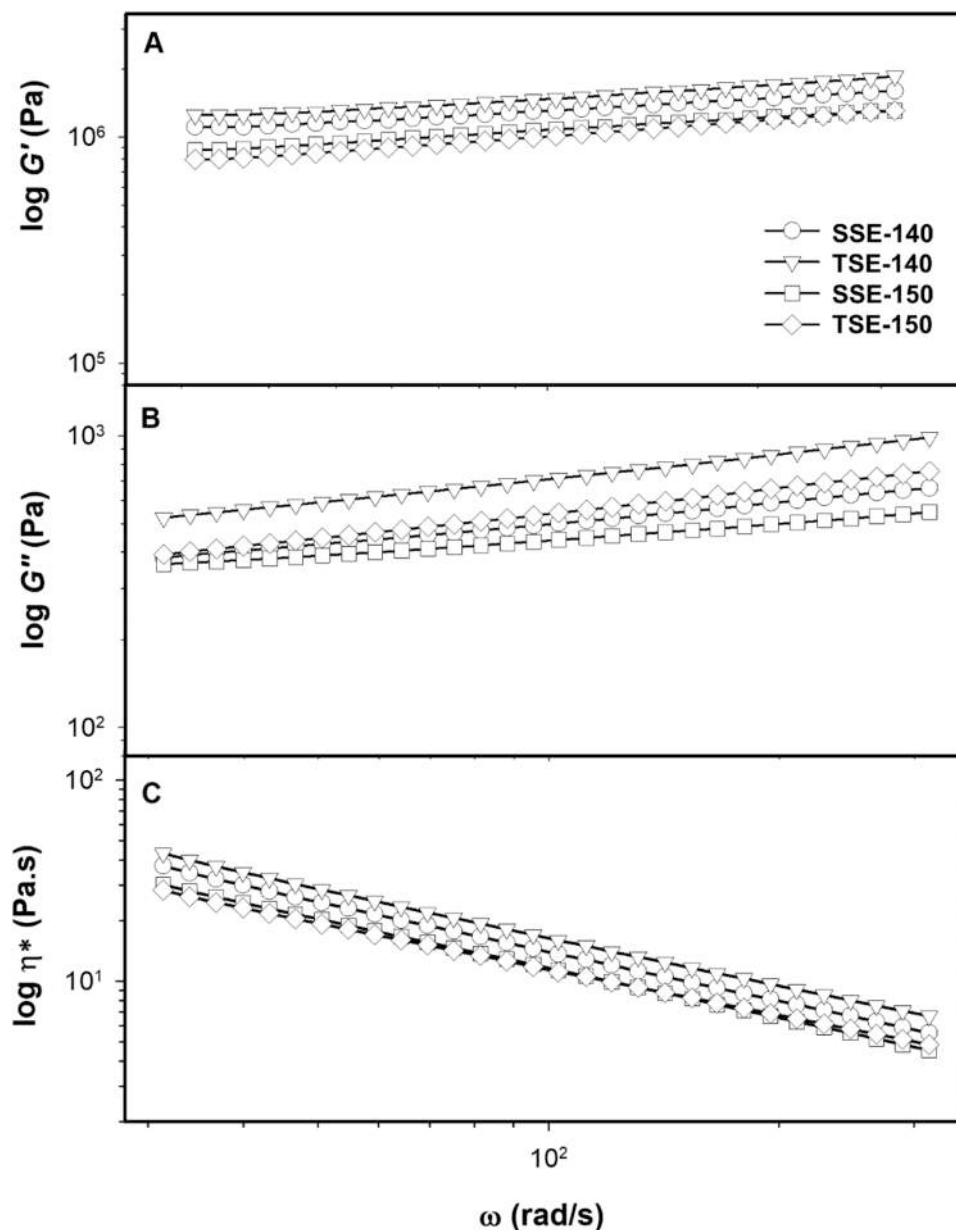


Fig. 6. Effect of angular frequency (ω) and temperature (140 and 150 °C) on storage modulus (G'), loss modulus (G''), and complex viscosity (η^*) of the TPAS/SF biocomposites compounded by SSE and TSE.

temperature increased, η^* decreased and that the values of η^* evaluated at 140 °C of the biocomposite compounded in the TSE were higher than the one compounded in the SSE, as observed for G' and G'' .

3.6. Mechanical properties

Fig. 7 shows the stress-strain curves of bioplastics. All the curves presented a characteristic behavior of thermoplastic starches, presenting two specific regions regardless of the processes. At low strains, stress increased linearly and showed a slope indicating chains' resistance against returnable deformation in the elastic region. At high strains, a non-linear behavior occurred with extensive ductile or plastic deformation until failure occurred (González-Seligra et al., 2017; Ochoa-Yepes et al., 2019).

Analyzing the effect of the compounding processes, it was observed that, in general, the biocomposites compounded by TSE presented higher ductility and stiffness than the ones compounded in SSE. This

behavior could be related to the better distribution of SF in TPAS in the biocomposites compounded by TSE and matrix-fiber adhesion (Pickering et al., 2016). This behavior is supported by the results obtained in SEM (Fig. 4B and D) since it is appreciated that samples compounded by a TSE showed better fiber distribution.

From the point of view of the manufacturing process, it is important to mention that just the samples prepared by compression and injection molding are directly comparable because the thickness of the specimens obtained was between 2 and 3 mm. In contrast, films of the TPAS/SF biocomposites obtained by FF were about 0.5 mm thick. It has been reported that the thickness of samples affects the mechanical performance of polymers (Jansson and Thuvander, 2004; Uribe-Arocha et al., 2003). As expected, in this work, samples prepared by injection molding showed higher tensile resistance and elongation at break than those prepared by compression (Fig. 7). Chodak et al. (2001) suggested that the better performance of composite materials prepared by injection molding is produced by both the additional mixing that produced a better dispersion and the orientation due to elongational flow during the

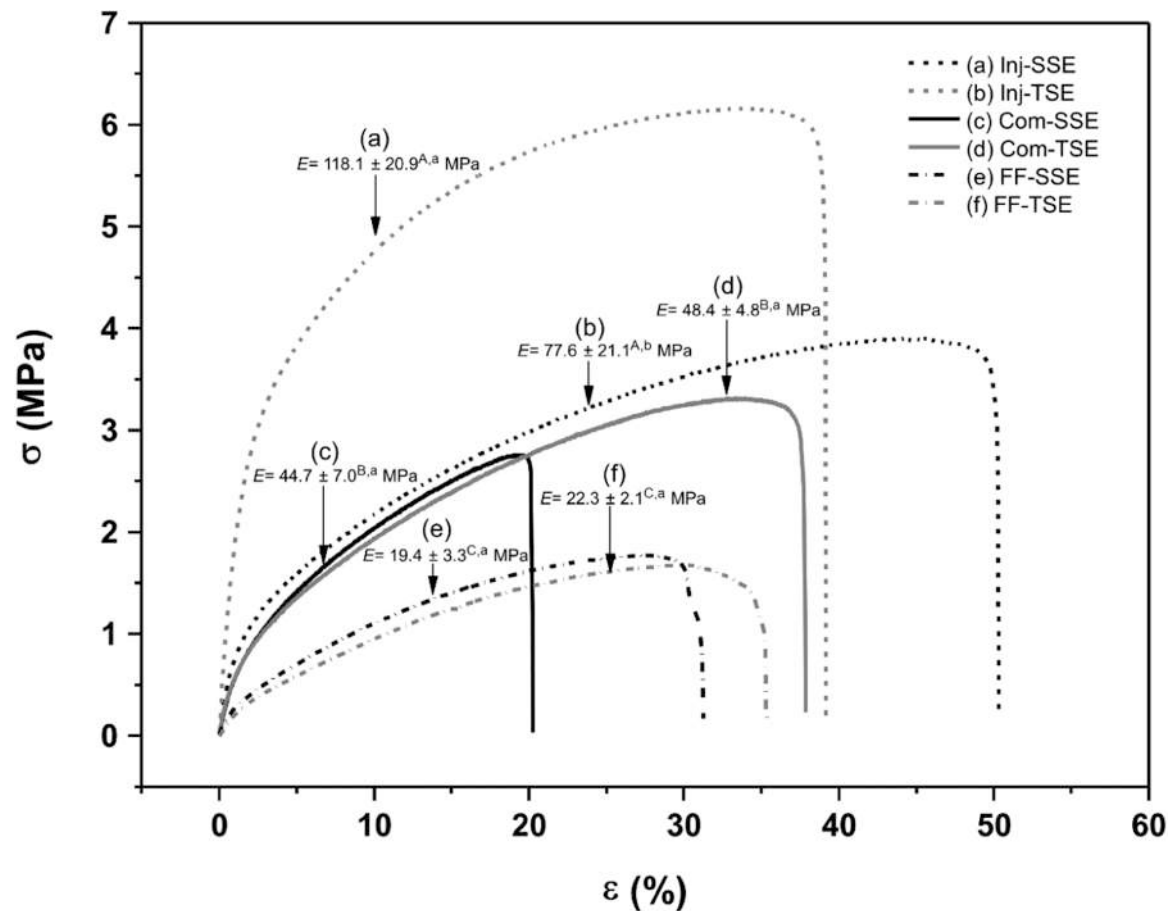


Fig. 7. Stress-Strain curves of TPAS/SF biocomposites compounded by SSE and TSE and processed by Inj, Com, and FF. Different uppercase letters (A, B, C) and lowercase letters (a, b, c) show statistical differences ($P \leq 0.05$) among treatments according to the Tukey test for the compounding process and plastic processing methods, respectively. E = Young modulus.

injection molding process.

It is well known that, on the one hand, long fibers promote a higher reinforcement effect than shorter fibers and, on the other hand, as better the homogeneity of fibers in a polymeric matrix as higher the reinforcement effect. It seemed that in the balance of fiber length and fiber distribution, the latter had a higher effect on the stress-strain curves and resulted in tougher injected biocomposites. This behavior is sustained with the observed by SEM. Fig. 4 shows that the second heating and shearing treatment applied to the TPAS/SF biocomposites during Inj processing resulted in a reduction of the fiber size, but an improved distribution of shorter SF particles in the TPAS matrix compared to Com samples.

The biocomposites processed by FF, unexpectedly, showed lower stiffness and ductility than those prepared by the molding processes (Fig. 7). Jansson and Thuvander (2004) prepared TPS films from starch/glycerol (100:30) solutions with thicknesses from 0.3 to 2.5 mm, similar to this research. The authors observed that strain at break decreased from about 90–20% as the thickness of the films increased from 0.3 to 2.5 mm.

Inj-TSE recorded Young's modulus (E) of 118.1 ± 20.9 MPa, recording a significant difference ($P \leq 0.05$) regarding the other bioplastics by the effect of compounding and plastic processing method. Some authors have reported that TSE provides a more intensive mixing than SSE (Lenz et al., 2018; Pickering et al., 2016). Compounding by TSE could have promoted a suitable dispersion of the fibers, improving Young's modulus. Moreover, the high temperatures, shear stress, and pressure employed on the injection molding could have produced wear and decreased fibers' length, improving the strain and ductility of

bioplastics (Basiak et al., 2018; Li et al., 2018). Likewise, the injection process could have favored the starch molecular orientation and the intermolecular interactions between TPS and fibers (Lenz et al., 2018). For its part, Paiva et al. (2018) prepared TPS materials by melt mixing and injection molding, using 30% glycerol and reinforcing with 30% of starch/chitosan microparticles, obtaining an E of ≈ 80 MPa. Zanela et al. (2018), in injected materials of starch/polyvinyl alcohol reinforced with 10% oat fiber and 30% glycerol, obtained an E of ≈ 12 MPa. While Bortolatto et al. (2022) developed biocomposites of starch (50–75%), polyvinyl alcohol (6%), glycerol (25%), and soybean hull (4–19%), compounded by SSE and produced by thermoplastic injection. The authors reported an E range of 8–16.3 MPa. The E recorded in this study was higher than the reported in the literature for starch-based materials.

The behavior of Inj-TSE was unexpected since it is well known that when the stiffness increases, the elongation decreases. However, these specimens recorded a high Young's modulus. This material could be used in applications where high flexibilities are required without losing its strength.

3.7. Water solubility (WS) and contact angle (CA)

The analysis of WS of TPAS/SF biocomposites showed no defined trend on how the compounding and processing processes affected this property (Fig. 8A). Nonetheless, the WS values of TPAS/SF biocomposites were between 24.9% and 28.2%, which are lower than those reported in the literature for native starch-based biocomposites (≈ 30 –40%) (González-Seligra et al., 2017; Ochoa-Yepes et al., 2019; Zanela et al., 2018).

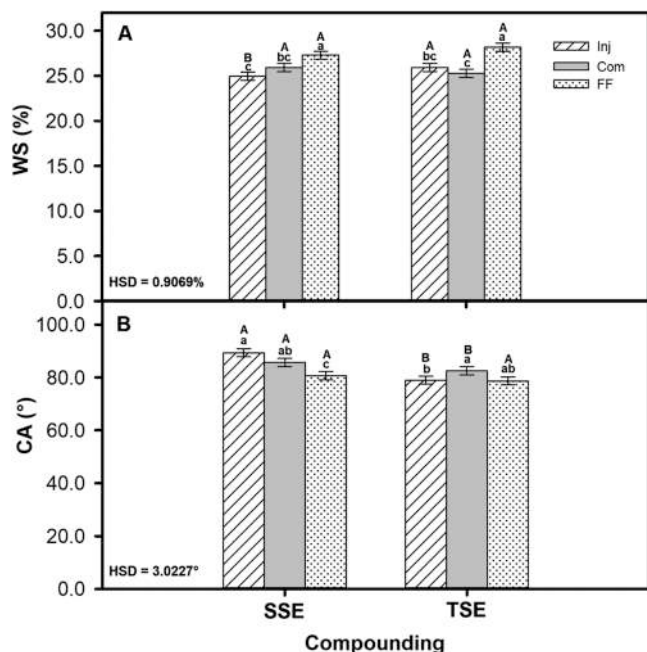


Fig. 8. Water solubility (WS) and contact angle (CA) of TPAS/SF biocomposites compounded by SSE and TSE and processed by Inj, Com, and FF. Different uppercase letters (A, B, C) show statistical differences ($P \leq 0.05$) among treatments for compounding process, and lowercase letters (a, b, c) show statistical differences ($P \leq 0.05$) among treatments for plastic processing methods, according to the Tukey test.

In a previous study, 18.5–24.7% solubility values for acetylated starch-based-biocomposites reinforced with modified sugarcane fiber produced from an SSE were obtained (Fitch-Vargas et al., 2019). In this work, an additional processing step was used to produce bioplastics, which was expected to obtain higher solubility values. However, these values did not increase considerably, suggesting that acetylated starch helped maintain the resistance to water (Colussi et al., 2017). Also, the fiber surface modification probably enhanced the interfacial adhesion between cellulose fibers and TPS, improving the barrier properties (Guimarães-de Farias et al., 2017; Satyanarayana et al., 2009).

The CA value corresponds to the initial contact between the material and a water droplet; a high value indicates higher surface hydrophobicity (Basiak et al., 2018; Li et al., 2018). The effect of compounding and processing methods on CA is shown in Fig. 8B. The CA of TPAS/SF biomaterials did not show a defined trend related to the compounding and processing processes, and the CA values varied from 78.0° to 89.3°. Li et al. (2018) obtained a CA of 71.7–81.6° in native starch and cellulose nanofibers films, while Ochoa-Yepes et al. (2019) reported 67–68° in compressed native starch materials with lentil protein. The values obtained in this study are higher than those reported in the literature, which could be due to the presence of hydrophobic acetyl groups in TPAS (Colussi et al., 2017; Wang et al., 2014).

Inj-SSE recorded the highest CA (89.3°), indicating that water absorption was not favored. It is known that injection molding produces more significant mechanical damage and better molecular orientation, improving interfacial adhesion, which probably enhances water resistance (Basiak et al., 2018; Li et al., 2018). Interestingly, the biocomposites having the highest CA values (more hydrophobic) had the lowest WS values, such as Inj-SSE. It seemed that the WS values were dependent on the surface hydrophobicity of TPAS/SF biocomposites.

3.8. Biodegradability

Fig. 9 shows weight loss (WL) evolution after 35 days of exposition to soil burial of TPAS/SF biocomposites compounded by SSE and TSE and

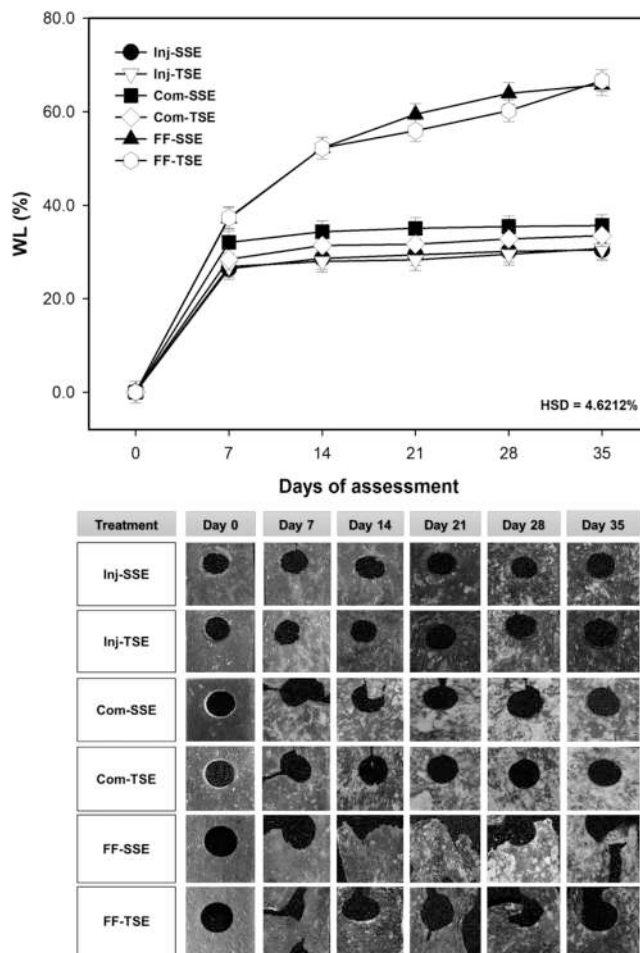


Fig. 9. Biodegradability of TPAS/SF biocomposites compounded by SSE and TSE and processed by Inj, Com, and FF.

processed by Inj, Com, and FF. After seven days of the assay, the bioplastics recorded a weight reduction between 26% and 38%. This behavior may be due to the extraction of lower molecular weight compounds such as glycerol, sugars, and starch oligomers (Tena-Salcido et al., 2008).

The bioplastics showed no defined behavior on how the compounding stage affected the WL. Contrariwise, the processing stage did significantly influence. FF specimens recorded the highest WL from day 14 to the end of the assay, showing a significant difference ($P \leq 0.05$) regarding Inj and Com. This phenomenon seemed to be dependent on the thickness of the bioplastic specimens, i.e., flat films having a thickness of about 0.5 mm lost 38% of the initial mass, while injection specimens having around 3 mm of thickness lost only 26% during the same period (Altskär et al., 2008; Tena-Salcido et al., 2008). Bertuzzi et al. (2007) report that water absorption depends on the thickness of starch films at high RH. Thus, under the conditions of the WL assay, the water content probably began to increase exponentially, swelling the TPAS matrix and facilitating water transport and disaggregation in FF bioplastics. The results for FF are supported by the obtained in WS (highest values) and CA (lowest values).

After day seven of analysis, the evolution of WL of flat films showed a slower but constant weight reduction, while the injection and compression molded biomaterials tended to stabilize. According to SEM micrographs, injected and compressed materials kept a more compact polymeric matrix than flat films. These materials, having a denser structure, could have avoided the TPS swelling and the plasticizer and starch molecules' diffusion.

Also, Fig. 9 shows morphology changes on the sample's surface. All

specimens showed changes in color from brown to yellow, probably caused by the glycerol and matter loss (Tena-Salcido et al., 2008). Also, materials lost their original shape showing an irregular and rough surface with some cracks. After seven days of exposition to soil burial, FF specimens showed fragmentation, which could be responsible for the higher rate of WL of the thinner samples.

4. Conclusion

It was possible to successfully obtain TPAS/SF biocomposites compounded by SSE and TSE and processed by Inj, Com, and FF. The bioplastics' characterization verified that compounding by TSE resulted in a significant decrease in the fiber length but a more homogeneous distribution of SF in the TPAS matrix than SSE. Moreover, the TPAS/SF biocomposites processing by Inj reduced the fibers' length and improved the SF particles' distribution. The combination of compounding by TSE and processing by Inj resulted in the toughest behavior in tensile tests of the TPAS/SF biocomposites evaluated in this work.

The solubility of all materials ranged between 24.9% and 28.2%, which is lower than the WS reported for native starch-based biocomposites. It is probably that chemically modified raw materials maintained low solubility values despite compounding and processing. Bioplastics recorded a WL of 30–66% in 35 days of the assay. This suggests that biomaterials will disintegrate and biodegrade under compost conditions in a shorter time than that reported for conventional plastics. Hence, depending on the practical application (food services, packaging applications, agriculture, among others), TPAS/SF bioplastics developed on an industrial scale could be an alternative to synthetic plastics to reduce the damage caused to the environment.

Formatting of funding sources

This research did not receive any specific grant from funding agencies in the public, commercial, or not-for-profit sectors.

CRediT authorship contribution statement

All the authors participated in the preparation of this paper. **Fitch-Vargas**: Conceptualization, Methodology, Validation, Investigation, Writing – original draft. **Rodríguez-González**: Formal analysis, Writing – review & editing, Visualization, Supervision. **Camacho-Hernández**: Resources, Funding acquisition, Formal analysis. **Martínez-Bustos**: Resources, Writing – review & editing. **Calderón-Castro**: Formal analysis, Investigation. **Zazueta-Morales**: Writing – review & editing, Visualization. **Aguilar-Palazuelos**: Conceptualization, Validation, Supervision, Project administration.

Declaration of Competing Interest

The authors declare that they have no known competing financial interests or personal relationships that could have appeared to influence the work reported in this paper.

Data availability

Data will be made available on request.

Acknowledgments

The authors thank Jesús Rodríguez, Rodrigo Cedillo, and Mario Palacios from the Polymer Processing Laboratory of CIQA for compounding and processing bioplastics and mechanical and rheological testing and to CINVESTAV for mechanical and microstructural analysis techniques.

Appendix A. Supporting information

Supplementary data associated with this article can be found in the online version at doi:10.1016/j.indcrop.2022.116084.

References

- Albrektsson, T., Wennerberg, A., 2004. Oral implant surfaces: Part 1—review focusing on topographic and chemical properties of different surfaces and in vivo responses to them. *Int. J. Prosthodont.* 17 (5), 536–543.
- Altskär, A., Andersson, R., Boldizar, A., Koch, K., Stading, M., Rigdahl, M., Thunwall, M., 2008. Some effects of processing on the molecular structure and morphology of thermoplastic starch. *Carbohydr. Polym.* 71 (4), 591–597. <https://doi.org/10.1016/j.carbpol.2007.07.003>.
- Alves-Da Silva, J.B., Suman-Bretas, R.E., Almeida-Lucas, A., Marini, J., Bruna-Da Silva, A., Santos-Santana, J.S., et al. Druzian, J.I., 2020. Rheological, mechanical, thermal, and morphological properties of blends poly (butylene adipate-co-terephthalate), thermoplastic starch, and cellulose nanoparticles. *Polymer Engineering & Science*, 60(7), 1482–1493. <https://doi.org/10.1002/pen.25395>.
- Amin, M.R., Chowdhury, M.A., Kowser, M.A., 2019. Characterization and performance analysis of composite bioplastics synthesized using titanium dioxide nanoparticles with corn starch. *Heliyon* 5 (8), e02009. <https://doi.org/10.1016/j.heliyon.2019.e02009>.
- Bajpai, A.K., Goswami, A., Bajpai, J., Sinha, B.K., 2018. Study of mechanical, optical, and electrical behaviors of calcium alginate/poly (vinyl alcohol)–vanadium pentoxide bionanocomposite films. *Macromol. Res.* 26 (4), 305–316. <https://doi.org/10.1007/s13233-018-6040-0>.
- Basiak, E., Lenart, A., Debeaufort, F., 2018. How glycerol and water contents affect the structural and functional properties of starch-based edible films. *Polymers* 10 (4), 412. <https://doi.org/10.3390/polym10040412>.
- Bertuzzi, M.A., Armada, M., Gottifredi, J.C., 2007. Physicochemical characterization of starch based films. *J. Food Eng.* 82 (1), 17–25. <https://doi.org/10.1016/j.jfoodeng.2006.12.016>.
- Bortolato, R., Bittencourt, P.R.S., Yamashita, F., 2022. Biodegradable starch/polyvinyl alcohol composites produced by thermoplastic injection containing cellulose extracted from soybean hulls (*Glycine max* L.). *Ind. Crops Prod.* 176, 114383 <https://doi.org/10.1016/j.indcrop.2021.114383>.
- Cao, Y., Shibata, S., Fukumoto, I., 2006. Mechanical properties of biodegradable composites reinforced with bagasse fibre before and after alkali treatments. *Compos. Part A: Appl. Sci. Manuf.* 37 (3), 423–429. <https://doi.org/10.1016/j.compositesa.2005.05.045>.
- Castillo, L.A., López, O.V., García, M.A., Barbosa, S.E., Villar, M.A., 2019. Crystalline morphology of thermoplastic starch/talc nanocomposites induced by thermal processing. *Heliyon* 5 (6), e01877. <https://doi.org/10.1016/j.heliyon.2019.e01877>.
- Chaves da Silva, N.M., Fakhouri, F.M., Fialho, R.L.L., Cabral-Albuquerque, E.C. d. M., 2018. Starch-recycled gelatin composite films produced by extrusion: Physical and mechanical properties. *J. Appl. Polym. Sci.* 135 (19), 46254. <https://doi.org/10.1002/app.46254>.
- Chodak, I., Omastova, M., Pionteck, J., 2001. Relation between electrical and mechanical properties of conducting polymer composites. *J. Appl. Polym. Sci.* 82 (8), 1903–1906. <https://doi.org/10.1002/app.2035>.
- Colussi, R., Zanella-Pinto, V., El Halal, S.L.M., Biduski, B., Prietto, L., Dufech-Castilhos, D., et al. Guerra-Dias, A. R. (2017). Acetylated rice starches films with different levels of amylose: Mechanical, water vapor barrier, thermal, and biodegradability properties. *Food Chemistry*, 221, 1614–1620. <https://doi.org/10.1016/j.foodchem.2016.10.129>.
- Fitch-Vargas, P.R., Camacho-Hernández, I.L., Martínez-Bustos, F., Islas-Rubio, A.R., Carrillo-Cañedo, K.L., Calderón-Castro, A., et al. Aguilar-Palazuelos, E. (2019). Mechanical, physical and microstructural properties of acetylated starch-based biocomposites reinforced with acetylated sugarcane fiber. *Carbohydrate Polymers*, 219, 378–386. <https://doi.org/10.1016/j.carbpol.2019.05.043>.
- Fowler, P.A., Hughes, J.M., Elias, R.M., 2006. Biocomposites: technology, environmental credentials and market forces. *J. Sci. Food Agric.* 86 (12), 1781–1789. <https://doi.org/10.1002/jsfa.2558>.
- González-Seligra, P., Medina-Jaramillo, C., Famá, L., Goyanes, S., 2016. Biodegradable and non-retrogradable eco-films based on starch–glycerol with citric acid as crosslinking agent. *Carbohydr. Polym.* 138, 66–74. <https://doi.org/10.1016/j.carbpol.2015.11.041>.
- González-Seligra, P., Guz, L., Ochoa-Yepes, O., Goyanes, S., Famá, L., 2017. Influence of extrusion process conditions on starch film morphology. *LWT-Food Sci. Technol.* 84, 520–528. <https://doi.org/10.1016/j.lwt.2017.06.027>.
- Guimaraes-de Farias, J.G., Cordeiro-Cavalcante, R., Rodrigues-Canabarro, B., Magalhães-Viana, H., Scholz, S., Simão, R.A., 2017. Surface lignin removal on coir fibers by plasma treatment for improved adhesion in thermoplastic starch composites. *Carbohydr. Polym.* 165, 429–436. <https://doi.org/10.1016/j.carbpol.2017.02.042>.
- Gurunathan, T., Mohanty, S., Nayak, S.K., 2015. A review of the recent developments in biocomposites based on natural fibres and their application perspectives. *Compos. Part A: Appl. Sci. Manuf.* 77, 1–25. <https://doi.org/10.1016/j.compositesa.2015.06.007>.
- Huang, L., Zhao, H., Yi, T., Qi, M., Xu, H., Mo, Q., et al., 2020. Preparation and Properties of Cassava Residue Cellulose Nanofibril/Cassava Starch Composite Films (Liu, Y.). *Nanomaterials* 10 (4), 755. <https://doi.org/10.3390/nano10040755>.
- Ibrahim, H., Mehanny, S., Darwish, L., Farag, M., 2018. A comparative study on the mechanical and biodegradation characteristics of starch-based composites reinforced

- with different lignocellulosic fibers. *J. Polym. Environ.* 26 (6), 2434–2447. <https://doi.org/10.1007/s10924-017-1143-x>.
- Jansson, A., Thuvander, F., 2004. Influence of thickness on the mechanical properties for starch films. *Carbohydr. Polym.* 56 (4), 499–503. <https://doi.org/10.1016/j.carbpol.2004.03.019>.
- Jeon, Y.S., Lowell, A.V., Gross, R.A., 1999. Studies of starch esterification: reactions with alkenylsuccinates in aqueous slurry systems. *Starch-Stärke* 51 (2-3), 90–93. [https://doi.org/10.1002/\(SICI\)1521-379X\(199903\)51:2<90::AID-STAR90>3.0.CO;2-M](https://doi.org/10.1002/(SICI)1521-379X(199903)51:2<90::AID-STAR90>3.0.CO;2-M).
- Jumaidin, R., Sapuan, S.M., Jawaid, M., Ishak, M.R., Sahari, J., 2017. Thermal, mechanical, and physical properties of seaweed/sugar palm fibre reinforced thermoplastic sugar palm starch/agar hybrid composites. *Int. J. Biol. Macromol.* 97, 606–615. <https://doi.org/10.1016/j.ijbiomac.2017.01.079>.
- Kaith, B.S., Jindal, R., Jana, A.K., Maiti, M., 2010. Development of corn starch based green composites reinforced with *Saccharum spontaneum* L fiber and graft copolymers—Evaluation of thermal, physico-chemical and mechanical properties. *Bioresour. Technol.* 101 (17), 6843–6851. <https://doi.org/10.1016/j.biortech.2010.03.113>.
- Kim, N.K., Lin, R.J.T., Bhattacharyya, D., 2014. Extruded short wool fibre composites: mechanical and fire retardant properties. *Compos. Part B: Eng.* 67, 472–480. <https://doi.org/10.1016/j.compositesb.2014.08.002>.
- Lenz, D.M., Tedesco, D.M., Camani, P.H., dos Santos Rosa, D., 2018. Multiple reprocessing cycles of corn starch-based biocomposites reinforced with Curauá fiber. *J. Polym. Environ.* 26 (7), 3005–3016. <https://doi.org/10.1007/s10924-018-1179-6>.
- Li, M., Tian, X., Jin, R., Li, D., 2018. Preparation and characterization of nanocomposite films containing starch and cellulose nanofibers. *Ind. Crops Prod.* 123, 654–660. <https://doi.org/10.1016/j.indcrop.2018.07.043>.
- Li, S., Wang, J., Qu, W., Cheng, J., Lei, Y., Wang, D., Zhang, F., 2020. Green synthesis and properties of an epoxy-modified oxidized starch-grafted styrene-acrylate emulsion. *Eur. Polym. J.* 123, 109412. <https://doi.org/10.1016/j.eurpolymj.2019.109412>.
- Li, X., Tabil, L.G., Panigrahi, S., 2007. Chemical treatments of natural fiber for use in natural fiber-reinforced composites: a review. *J. Polym. Environ.* 15 (1), 25–33. <https://doi.org/10.1007/s10924-006-0042-3>.
- Maldonado-García, M.A., Hernández-Toledo, U.I., Montes-García, P., Valdez-Tamez, P.L., 2018. The influence of untreated sugarcane bagasse ash on the microstructural and mechanical properties of mortars. *Mater. De. Constr.* 68 (329), 148. <https://doi.org/10.3989/mc.2018.13716>.
- Mandal, A., Chakrabarty, D., 2011. Isolation of nanocellulose from waste sugarcane bagasse (SCB) and its characterization. *Carbohydr. Polym.* 86 (3), 1291–1299. <https://doi.org/10.1016/j.carbpol.2011.06.030>.
- Mohan, C.C., Harini, K., Karthikeyan, S., Sudharsan, K., Sukumar, M., 2018. Effect of film constituents and different processing conditions on the properties of starch based thermoplastic films. *Int. J. Biol. Macromol.* 120, 2007–2016. <https://doi.org/10.1016/j.ijbiomac.2018.09.161>.
- Motaung, T.E., Anandjiwala, R.D., 2015. Effect of alkali and acid treatment on thermal degradation kinetics of sugar cane bagasse. *Ind. Crops Prod.* 74, 472–477. <https://doi.org/10.1016/j.indcrop.2015.05.062>.
- Ochoa-Yepes, O., Di Gioglio, L., Goyanes, S., Mauri, A., Famá, L., 2019. Influence of process (extrusion/thermo-compression, casting) and lentil protein content on physicochemical properties of starch films. *Carbohydr. Polym.* 208, 221–231. <https://doi.org/10.1016/j.carbpol.2018.12.030>.
- Olagunju, A.I., Omoba, O.S., Enujiugha, V.N., Wiens, R.A., Gough, K.M., Aluko, R.E., 2020. Influence of acetylation on physicochemical and morphological characteristics of pigeon pea starch. *Food Hydrocoll.* 100, 105424. <https://doi.org/10.1016/j.foodhyd.2019.105424>.
- Paiva, D., Pereira, A., Pires, A., Martins, J., Carvalho, L., Magalhães, F., 2018. Reinforcement of thermoplastic corn starch with crosslinked starch/chitosan microparticles. *Polymers* 10 (9), 985. <https://doi.org/10.3390/polym10090985>.
- Pickering, K.L., Efenfy, M.G.A., Le, T.M., 2016. A review of recent developments in natural fibre composites and their mechanical performance. *Compos. Part A: Appl. Sci. Manuf.* 83, 98–112. <https://doi.org/10.1016/j.compositesa.2015.08.038>.
- Raquez, J.M., Nabar, Y., Srinivasan, M., Shin, B.Y., Narayan, R., Dubois, P., 2008. Maleated thermoplastic starch by reactive extrusion. *Carbohydr. Polym.* 74 (2), 159–169. <https://doi.org/10.1016/j.carbpol.2008.01.027>.
- Rico, M., Rodríguez-Llamazares, S., Barral, L., Bouza, R., Montero, B., 2016. Processing and characterization of polyols plasticized-starch reinforced with microcrystalline cellulose. *Carbohydr. Polym.* 149, 83–93. <https://doi.org/10.1016/j.carbpol.2016.04.087>.
- Rodríguez-González, F.J., Ramsay, B.A., Favis, B.D., 2004. Rheological and thermal properties of thermoplastic starch with high glycerol content. *Carbohydr. Polym.* 58 (2), 139–147. <https://doi.org/10.1016/j.carbpol.2004.06.002>.
- Satyanarayana, K.G., Arizaga, G.G.C., Wypych, F., 2009. Biodegradable composites based on lignocellulosic fibers—An overview. *Prog. Polym. Sci.* 34 (9), 982–1021. <https://doi.org/10.1016/j.progpolymsci.2008.12.002>.
- Taaca, K.L.M., Vasquez Jr, M.R., 2017. Fabrication of Ag-exchanged zeolite/chitosan composites and effects of plasma treatment. *Microporous Mesoporous Mater.* 241, 383–391. <https://doi.org/10.1016/j.micromeso.2017.01.002>.
- Tena-Salcido, C., Rodríguez-González, F., Méndez-Hernández, M., Contreras-Esquivel, J., 2008. Effect of morphology on the biodegradation of thermoplastic starch in LDPE/TPS blends. *Polym. Bull.* 60 (5), 677–688. <https://doi.org/10.1007/s00289-008-0903-0>.
- Uribe-Arocha, P., Mehler, C., Puskas, J.E. and Altstadt, V. (2003). Effect of sample thickness on the mechanical properties of injection-molded polyamide-6 and polyamide-6 clay nanocomposites. *Polymer*, 44(8), 2441–2446. <https://doi.org/10.1016/j.polymer.2003.08.002>.
- Van Soest, J.J.G., Hulleman, S.H.D., De Wit, D., Vliegthart, J.F.G., 1996. Crystallinity in starch bioplastics. *Ind. Crops Prod.* 5 (1), 11–22. [https://doi.org/10.1016/0926-6690\(95\)00048-8](https://doi.org/10.1016/0926-6690(95)00048-8).
- Wang, H., Kabir, M.M., Lau, K., 2014. Hemp reinforced composites with alkalization and acetylation fibre treatments. *Polym. Polym. Compos.* 22 (3), 247–251. <https://doi.org/10.1177/096739111402200304>.
- Wang, P., Chen, F., Zhang, H., Meng, W., Sun, Y., Liu, C., 2017. Large-scale preparation of jute fiber reinforced starch-based composites with high mechanical strength and optimized biodegradability. *Starch-Stärke* 69, 1700052. <https://doi.org/10.1002/star.201700052>.
- Zanela, J., Bilck, A.P., Casagrande, M., Grossmann, M.V.E., Yamashita, F., 2018. Oat fiber as reinforcement for starch/polyvinyl alcohol materials produced by injection molding. *Starch-Stärke* 70 (7–8), 1700248. <https://doi.org/10.1002/star.201700248>.